Nonlocal Heat Transport Due to Steep Temperature Gradients

J. F. Luciani and P. Mora
Centre de Physique Théorique de l'Ecole Polytechnique, F-91128 Palaiseau Cedex, France

and

J. Virmont
Laboratoire de Physique des Milieux Ionisés de l'Ecole Polytechnique, F-91128 Palaiseau Cedex, France
(Received 19 July 1983)

By comparison with fully kinetic Fokker-Planck calculations, a nonlocal macroscopic formula has been derived for the thermal heat flux. This formula leads in a physically relevant way to the saturation and the delocalization of the heat flux. Its introduction in a fluid code is straightforward and gives to some extent results comparable with classical flux-limited transport calculations with $f=0.1$. However, it also describes a significant level of preheating.

PACS numbers: 52.25.Fi, 44.10.+i, 52.50.Jm

A considerable amount of work has been recently devoted to the problem of electron heat transport down steep temperature gradients,[1-9] particularly in the context of laser-produced plasmas. The classical linear Spitzer-Härm (SH) theory[10] is limited to very small temperature gradients: $\lambda_0/L_t<2\ 10^{-3}$, where λ_0 is the electron mean free path for 90° scattering by electron and ion collisions, $\lambda_0=T_e^2/4\pi n_e(Z+1)e^4\times\ln\Lambda$, and L_t is the temperature scale length. For the steep temperature fronts occurring in laser-irradiated targets, results have been obtained by numerically solving the kinetic Fokker-Planck equation. In the hotter region of the heat front, the heat flux is observed to be several times smaller than the value given by the SH description, and is limited to a fraction ~0.1–0.2 of the free-streaming value $q_{FS}=n_e m_e v_e^3$, where $v_e=(T_e/m_e)^{1/2}$. On the contrary, at the base of the heat front, the conductivity exceeds the SH conductivity, because the flux has a nonlocal part due to the hot, nearly collisionless electrons streaming away from the top of the heat front.

Fluid codes describing laser-irradiated targets usually model the heat flux by a local law of the type

$$q=\min(q_{SH}, fq_{FS}), \tag{1}$$

where $q_{SH}=-\kappa\nabla T_e$ is the SH flux, and f is the flux-limit factor. However, as pointed out in previous works, this description is deficient in modeling heat transport in many respects, and particularly it cannot take into account its nonlocal character.

In this Letter, we propose a nonlocal expression for the heat flux. We demonstrate that it yields a good approximation to the actual heat flux, which we obtain from fully kinetic Fokker-Planck simulations. This expression is simple enough to be very easily tractable in a fluid code. The proposed expression is

$$q(x)=\int dx'\, q_{SH}(x')w(x,x'). \tag{2}$$

The kernel w is

$$w(x,x')=[2\lambda(x')]^{-1}\exp\left[-\left|\int_{x'}^{x} dx''\, n(x'')/\lambda(x')n(x')\right|\right], \tag{3}$$

where $\lambda(x')$ is an effective range for electrons of temperature $T_e(x')$. In terms of the mean free path $\lambda_0(x')$,

$$\lambda(x')=a(Z+1)^{1/2}\lambda_0(x'). \tag{4}$$

The constant a is adjusted by comparison with the results of our Fokker-Planck simulations: $a\simeq 32$.

Let us first show that the heat flux given by Eqs. (2)–(4) has several desirable properties. For gentle temperature and density gradients, $w(x,x')$ behaves like a δ function, with $\int dx'\, w(x,x')=1$, and the classical SH value is recovered. For a very steep temperature gradient and a uniform density, the exponential term in Eq. (3) can be approximated by 1 at the location of the temperature jump. By direct integration of Eq. (2), one obtains a maximum heat flux q_{max} which is a fraction of the free-streaming value q_{FS}. From the expression $q_{SH}=h(Z)(\lambda_0/L_t)q_{FS}$, with $h(Z)\simeq 64(2/\pi)^{1/2}(Z+0.24)/(Z+4.2)$, we get $q_{max}=[h(Z)/3a(Z+1)^{1/2}]q_{FS}$, which yields $q_{max}=0.12q_{FS}$ for $Z=5$. Finally, in contrast with Eq. (1), Eqs. (2)–

(4) are able to describe the nonlocal effect, because the heat flux value that they predict at position x depends on the whole temperature profile in a region around x of approximate size 2λ. This size has to be much larger than the mean free path λ_0 because the electrons involved in thermal transport have several times the thermal velocity, and also because they make $\sim(Z+1)$ scattering collisions before they lose energy due to a collision with a cold electron: This is accounted for by the factor $(Z+1)^{1/2}$, in agreement with the random-walk theory. It should be noted that the idea of using a convolution to express the heat flux was introduced in Ref. 6; however, the applicability of the kernel found there for linear ion sound waves to large thermal fronts was not tested.

Let us now demonstrate the good agreement of the flux predicted by Eqs. (2)–(4) with that obtained from fully kinetic Fokker-Planck simulations. The Fokker-Planck code used here has been described in Ref. 5. It uses a Legendre-polynomial expansion of the distribution function, with usually 4–6 terms. A self-consistent, implicitly calculated electric field ensures the zero-current condition. Reflective boundary conditions are used.

The electron equilibration time in a heat front is related to the electron mean collision time τ, and then is much shorter than the hydrodynamic time scale $\tau_{hyd}\sim L/c_s\sim(L/\lambda_0)(m_i/Zm_e)^{1/2}\tau$. The electron distribution then adiabatically follows the variation of the macroscopic quantities. Taking advantage of this time-scale separation, we run the code with fixed values of the collisional coefficients of the Fokker-Planck equation. Initial density and temperature profiles are chosen, typical of those found in laser-produced plasmas. The parallel diffusion coefficient $D_{\parallel}(x, v)$, the friction coefficient $C(x, v)$, and the angular diffusion coefficient $D_{\perp}(x, v)$ are then evaluated for these profiles, with a local Maxwellian shape for the isotropic part of the distribution function.

We observe that the distribution function $f(x, v, t)$ rather quickly reaches a steady state, in less than 100τ. In this steady state, the density profile $n_e(x)$ is essentially identical to the initial one. The temperature profile $T_e(x)$ is slightly different from the initial one. $f_0(x, v)$ is not a local Maxwellian: The main distortions are the depletion at high velocities in the hotter region, and to the contrary the presence of a hot tail in the colder region. These effects are similar to those observed in Fig. 3 of Ref. 9, though in our work the electron upscattering is only due to $D_{\parallel}$, while in Ref. 9 the upscattering is due to $D_{\parallel}$ and the laser heating term. The values of $D_{\parallel}$ and C evaluated with this f_0 would be somewhat different from those used in the simulation. These differences are not inconsistencies: They are, respectively, of the same order of magnitude as the two terms presently omitted in the simulation, namely, (1) the inverse bremsstrahlung heating due to the laser, which has essentially the shape of a velocity diffusion, i.e., which modifies $D_{\parallel}$ (at least if the laser intensity is not too large, $Zv_{laser}^2/v_e^2\ll 1$); and (2) the electron cooling due to the ion expansion, which has essentially the shape of a friction, i.e., which modifies C. The coefficient $D_{\perp}$, which depends very little on the shape of f_0, is unaffected. In conclusion, we consider that the steady state which is reached in our simulations is very relevant to the actual situation in the thermal front of a laser-irradiated target and in comprable problems.

Results of a typical simulation are shown in Fig. 1. The density and temperature profiles, chosen to resemble those found in laser plasmas, are shown in Fig. 1(a). However, the density ratio is smaller than in physical conditions. The horizontal coordinate ξ is the reduced position,

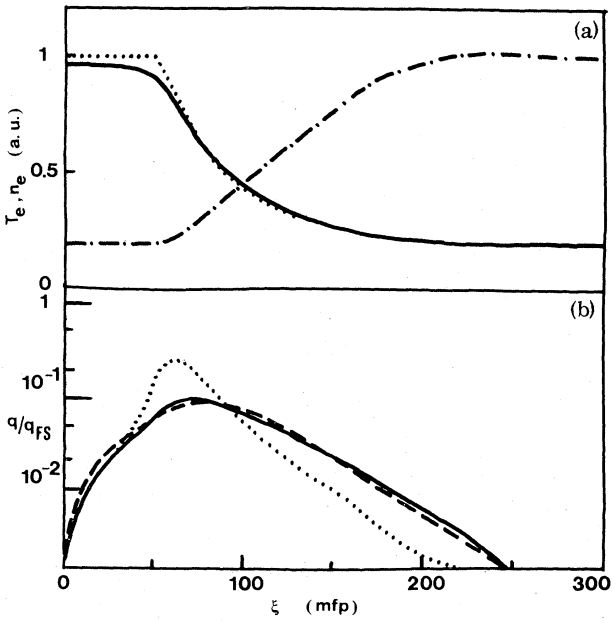

FIG. 1. (a) Initial (dotted line) and final (solid line) temperature profiles, and density profile (dash-dotted line). (b) Final heat-flux profiles, from the Fokker-Planck simulation (solid line), from SH law (dotted line), and from the delocalized model (dashed line).

defined with use of the mean free path of electrons at the hot temperature:

$$\xi = [\lambda_0(x_c) n_e(x_c)]^{-1} \int_0^x n_e(x')\,dx' .$$

The critical density (position x_c) would be at the edge of the hot region ($\xi = 50$), and the edge of the solid at the edge of the dense, cold region ($\xi = 230$). The thickness $\delta\xi = 180$ of the temperature front corresponds to a "rather short" laser pulse, since this is one third of the thickness (~ 540) which is reached by the ablation front in the long-time limit.[11] Note that the range $\delta\xi \sim 100$–500 is typical of the experimental conditions presently of interest. We observe that the initial temperature profile and the profile in the final steady state are close to each other. The difference would be even smaller for a thicker front.

Figure 1(b) compares three heat-flux profiles: the simulation result, the SH prediction, and the prediction of Eqs. (2)–(4). We observe that the SH expression overestimates the heat flux by a factor of 3 at the hot edge of the temperature front, while it underestimates the flux by a factor of 4 at the cold edge. To the contrary, our expression fits the simulation result much more closely along the whole profile: the difference everywhere is less than 25%. Note that the use of Eq. (1) would yield an improvement over the value at the hot edge[5]; however, it would leave uncorrected the large discrepancy present at the cold edge. The fact that our expressions (2)–(4) strongly improve on the SH value all along the profile is due to the fact that they incorporate the unique cause of the breakdown of SH model: the delocalization of the heat flux.

Other simulations have been run with various conditions: smoother gradients, or steeper gradients; isobaric, or isodensity systems. We have also used different values of Z. It is remarkable that the same value of a (~ 30–35) always gives a good fit in the conduction layer. A larger density ratio should not change the results, at least in a quasi-isobaric situation, since in the high-density layer, the upscattering is negligible, while the density dependence of the friction has been taken into account in the kernel w.

In the corona, the agreement between the simulation and the proposed heat-flux formula is not always as good as in Fig. 1, in particular when the density decreases in the corona. The disagreement is also observed with the SH formula as well. In fact we do not expect any such formula to be realistic in the collisionless corona, where the electron mean collision time becomes comparable with the hydrodynamic time scale.

Finally, we have introduced Eqs. (2)–(4) in a fluid code describing the laser-plasma interaction, the one-dimensional Lagrangian code FILM.[12] In the underdense plasma, Eqs. (2)–(4) cannot describe the collisionless outward heat flow necessary to maintain the nearly isothermal plasma expansion in vacuum.[13] Thus we have forced a constant temperature in the corona. The numerical implementation of Eq. (2) can be done as follows: For each cell, one distinguishes its own contribution to the integral, and the contribution of the other cells. The former is treated by the usual implicit scheme, and is taken into account by properly reducing the local conductivity. The latter is treated as an explicit term, exactly as one does for suprathermal-electron energy deposition. The numerical stability of the procedure can be demonstrated. Figure 2 corresponds to a typical run: A Gaussian pulse (1.06 μm, 150 psec full width at half maximum, $P_{max} = 2 \times 10^{14}$ W cm^{-2}) irradiates an aluminum target, treated with a perfect-gas equation of state. Energy is absorbed by classical inverse bremsstrahlung. This leads to a slight overestimation of the absorption, and of the transport itself,[9,14] which we neglect here, according to the condition $Zv_{laser}^2/v_e^2 < 1$. The code has been run with Eqs. (2)–(4), or with Eq. (1) and various values of the flux-limit parameter f. To some extent Eqs. (2)–(4) and Eq. (1) with $f = 0.10$ give similar results: in particular, the temperature in the corona and at

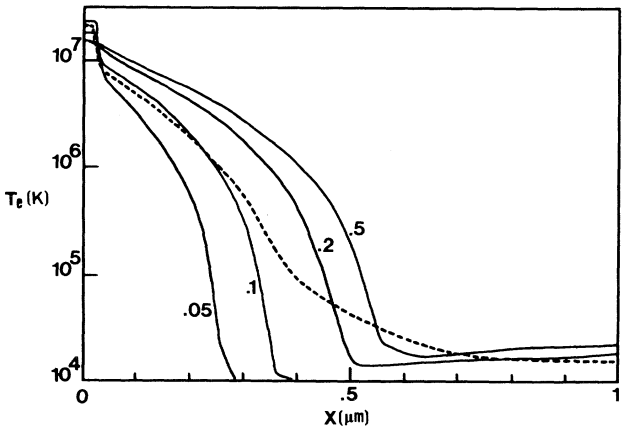

FIG. 2. Temperature profiles in Lagrangian coordinates from the fluid code FILM. Time is 50 psec after the peak of the laser pulse. Dashed line: the delocalized heat flux [Eqs. (2)–(4)] is used; solid lines: classical flux-limited heat flux [Eq. (1)] is used, with various values of the "flux-limit" factor f.

the top of the heat front, the total absorption, the ablation pressure, and consequently the shock properties. However, the temperature profiles are quite different in the intermediate region ($1 < T_e < 50$ eV) because of the preheating. As a result, this smoothing of the ablation front might considerably affect the hydrodynamic instabilities always present in this region. Note that the precursor foot of Fig. 2 can be compared to the corresponding result of Mason.[4]

The value $f = 0.10$ seems in agreement with the results of Wyndham *et al.*[15] and Goldsack *et al.*[16] On the other hand, the value $f = 0.03$ observed in other experiments[17] would require a value roughly 3 times larger, which does not seem possible in the frame of our one-dimensional, turbulence-free theory.

In conclusion, the expression of the heat flux given by Eqs. (2)–(4) describes fairly well the heat transport in a steep temperature gradient. It both correctly describes the inhibited heat flux on the main body of the heat front, and correctly predicts the preheating at the base of the heat front. Finally, the additional computer cost of using Eqs. (2)–(4) instead of Eq. (1) in a fluid code is negligible.

The Centre de Physique Théorique de l'Ecole Polytechnique is Groupe de Recherche du Centre National de la Recherche Scientifique No. 48.

[1]D. R. Gray and D. J. Kilkenny, Plasma Phys. 22, 81 (1980).

[2]A. R. Bell, R. G. Evans, and D. J. Nicholas, Phys. Rev. Lett. 46, 243 (1981).

[3]D. Shvarts, J. Delettrez, R. L. McCrory, and C. P. Verdon, Phys. Rev. Lett. 47, 247 (1981).

[4]R. J. Mason, Phys. Rev. Lett. 47, 652 (1981).

[5]J. P. Matte and J. Virmont, Phys. Rev. Lett. 49, 1936 (1982); J. P. Matte and J. Virmont, in Report on the Centre Européan de Calcul Atomique et Moléculaire Workshop on the Flux Limiter and Heat Flow Instabilities, 14 September–2 October 1981, Orsay, France (unpublished).

[6]A. R. Bell, Phys. Fluids 26, 279 (1983).

[7]D. J. Bond, Phys. Lett. 88A, 144 (1982).

[8]S. A. Khan and T. D. Rognlien, Phys. Fluids 24, 1442 (1981).

[9]J. R. Albritton, Phys. Rev. Lett. 50, 2078 (1983).

[10]L. Spitzer and R. Härm, Phys. Rev. 89, 977 (1953).

[11]J. L. Bobin, Phys. Fluids 14, 2341 (1971).

[12]J. Virmont, R. Pellat, and P. Mora, Phys. Fluids 21, 567 (1978); D. Shvarts, C. Jablon, I. B. Bernstein, J. Virmont, and P. Mora, Nucl. Fusion 19, 1457 (1979).

[13]P. Mora and R. Pellat, Phys. Fluids 22, 2300 (1979); J. Denavit, Phys. Fluids 22, 1384 (1979).

[14]A. B. Langdon, Phys. Rev. Lett. 44, 575 (1980); P. Mora and H. Yahi, Phys. Rev. A 26, 2259 (1982).

[15]E. S. Wyndham, J. D. Kilkenny, H. H. Chuaqui, and A. K. L. Dymoke-Bradshaw, J. Phys. D 15, 1683 (1982).

[16]T. J. Goldsack *et al.*, Phys. Fluids 25, 1634 (1982).

[17]W. C. Mead *et al.*, Phys. Rev. Lett. 47, 1289 (1981); R. Fabbro *et al.*, Phys. Rev. A 26, 2289 (1982).